

Time Series-Based Load Flow Simulation Algorithm for Distributed Generation in Distribution Networks [†]

Swathi Tangi ¹, D. N. Gaonkar ², A. S. Veerendra ^{1,*}  and R. Shivarudraswamy ¹

¹ Department of Electrical and Electronics Engineering, Manipal Institute of Technology, Manipal Academy of Higher Education, Manipal 576104, Karnataka, India; swathi.tangi@manipal.edu (S.T.); shivarudraswamy.r@manipal.edu (R.S.)

² Department of Electrical and Electronics Engineering, National Institute of Technology Karnataka (NITK), Surathkal 575025, Karnataka, India; dngaonkar@nitk.edu.in

* Correspondence: veerendra.babu@manipal.edu; Tel.: +91-9866489185

[†] Presented at the International Conference on Electronics, Engineering Physics and Earth Science (EEPES'24), Kavala, Greece, 19–21 June 2024.

Abstract: This paper proposes a load flow model to estimate the actual power output by incorporating time series data for solar irradiance and wind speed at a specific location. The integration of this time series data into the network is carried out in three distinct scenarios: considering only solar output, only wind output, and the combined contribution of solar and wind. These data integration processes are followed by load flow analysis conducted on the standard IEEE 33Bus radial distribution system. The time series simulations are executed using OpenDSS (Open Distribution System Simulator) software, which utilizes a COM (Common Object Model) interface to display results in MATLAB.

Keywords: distributed generation; OpenDSS; time series data; solar irradiance; wind speed

1. Introduction

Conventional power generation relies on predictable factors, while renewables face uncertainty due to weather variations. Algorithms integrating time series data into load flow analysis aid in scheduling renewable generation more effectively. This approach optimizes renewable source usage and provides insight into resource availability at specific locations. Ultimately, it enhances the reliability and efficiency of renewable energy systems [1,2].

Conventional load flow methods, like Newton–Raphson, are not suitable for radial distribution networks due to their high R/X ratio. Distribution system load flow (DSLFL) methods, developed for distribution automation, leverage radial network characteristics. Among these methods, forward–backward sweep algorithms are favored for their simplicity and speed in conducting distribution system load flow analysis [3]. One paper compares real power only and real power and reactive power simultaneously connected distributed generations in a 57-bus IEEE distribution test system using Matlab [4]. The authors of [5] propose a system for reducing active and reactive power losses in China’s distribution system and Yuan currency, aiming to minimize investment, operation, and line loss costs using distributed generation (DG) access.

This study examines the impact of distributed generation (DG) integration on protection systems and proposes mitigation methods based on previous research [6]. The paper introduces a power flow method for distribution networks that enhances accuracy, robustness, and computational efficiency by combining forward and backward sweeps without Jacobian matrix formation [7]. The paper introduces an improved harmony search algorithm for Distribution System Analysis (DPF), which can determine multiple power flow solutions for highly stressed conditions, overcoming limitations of previous techniques [8]. A study in Madrid found that grid-connected photovoltaic systems (GCPS) can affect low-voltage distribution networks’ performance due to power flow fluctuations,



Citation: Tangi, S.; Gaonkar, D.N.; Veerendra, A.S.; Shivarudraswamy, R. Time Series-Based Load Flow Simulation Algorithm for Distributed Generation in Distribution Networks. *Eng. Proc.* **2024**, *70*, 11. <https://doi.org/10.3390/engproc2024070011>

Academic Editor: Grigor Mihaylov

Published: 26 July 2024



Copyright: © 2024 by the authors. Licensee MDPI, Basel, Switzerland. This article is an open access article distributed under the terms and conditions of the Creative Commons Attribution (CC BY) license (<https://creativecommons.org/licenses/by/4.0/>).

influenced by penetration rates, distance, consumption and generation rates, and seasonal fluctuations [9].

The primary objectives of this proposed work are as follows:

1. Incorporate time series data for Photovoltaics (PV) within the distribution network to accurately model solar energy generation patterns.
2. Integrate time series data for wind energy within the distribution network to capture the variability and intermittency characteristic of wind power generation.
3. Develop a comprehensive framework for integrating time series data for both Photovoltaics and wind energy, accounting for their combined effects within the distribution network.

2. Methodology

2.1. Load Flow Algorithm and Optimal Dg Values

Distribution system load flow analysis cannot be performed using conventional techniques, like Newton Raphson and fast decoupled methods, because of high R/X ratio [10]. Backward and Forward sweep algorithm is used as a distribution load flow analysis tool.

The forward and backward sweep algorithm includes two steps:

1. Backward sweep includes the calculation of current flowing through each branch, crossing the network from end nodes toward the source nodes.
2. Forward sweep includes the calculation of voltage drop in each branch, crossing the network from source node towards the end nodes [11].

2.2. Particle Swarm Optimization (PSO)

Particle Swarm Optimization (PSO) is employed to connect distributed generation to the existing 33Bus network, aiming to minimize power loss and ensure bus voltages remain within limits. PSO, a metaheuristic search algorithm, is utilized as an efficient approach for solving complex network problems. Figure 1 illustrates the search process for optimal values, highlighting the iterative nature of PSO as a pathfinder in optimization processes, surpassing its subordinate heuristics, where: s^k is current searching point; s^{k+1} is modified searching point; v^k is current velocity; v^{k+1} is modified velocity of agent i ; V_{pbest} is velocity based on pbest (best objective function); and V_{gbest} is velocity based on gbest (global best objective function) [12]. Particle swarm optimization is applied to find the optimal location and size of DG with a non-unity power factor in variable load. Improved PSO has been developed, used to inject the active power and absorb the reactive power [13].

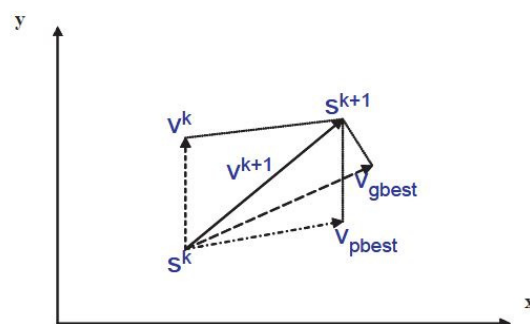


Figure 1. Concept of a searching point by PSO.

2.3. OpenDSS

OpenDSS, developed by EPRI, aids utilities in simulating feeders with distributed energy sources. Its COM interface allows results to be displayed on various platforms. Real-time simulations enable analysis of feeder models and prompt adjustments to equipment, addressing voltage fluctuations and harmonic distortions. Notably, OpenDSS can solve unbalanced radial feeders, enhancing its utility in power system analysis, as shown in Figure 2.

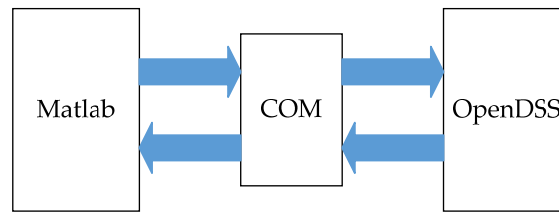


Figure 2. COM interface with MATLAB and OpenDss.

2.4. Methodology for Proposed PSO Technique

The PSO-based approach for solving the optimal placement of the DG problem to minimize real power loss is illustrated in Algorithm 1.

Algorithm 1. Optimal DG Placement Using PSO

- 1: **Input:** Line and bus data, as well as bus voltage limits
 - 2: **Output:** Optimal locations and sizes of DGs to minimize total real power loss.
 - 3: **Initialize:**
 - 4: Input line and bus data, along with bus voltage limits.
 - 5: Set iteration counter $k = 0$.
 - 6: Generate an initial population of particles with random positions and velocities, representing the sizes and locations of DGs.
 - 7: **Load Flow Calculation:**
 - 8: Determine the power loss using distribution load flow through the backward sweep–forward sweep method.
 - 9: **Particle Initialization:**
 - 10: **for** each particle **do**
 - 11: Check if bus voltages are within specified limits.
 - 12: **if** within limits **then**
 - 13: Assess the total power loss using Equation (1).
 - 14: **else**
 - 15: Mark the particle as infeasible.
 - 16: **end if**
 - 17: **end for**
 - 18: **Update Individual Best (Pbest):**
 - 19: **for** each particle **do**
 - 20: Compare the current objective value with the particle's Pbest.
 - 21: **if** the current objective value is lower **then**
 - 22: Update Pbest and record the particle's position.
 - 23: **end if**
 - 24: **end for**
 - 25: **Update Global Best (Gbest):**
 - 26: Identify the particle with the minimum Pbest among all particles.
 - 27: Set this minimum Pbest as the global best (Gbest).
 - 28: **Velocity and Position Update:**
 - 29: Update each particle's velocity using Equation (2).
 - 30: Update each particle's position using Equation (3).
 - 31: **Iteration Check:**
 - 32: **if** k reaches the maximum iteration limit **then**
 - 33: Proceed to Step 8.
 - 34: **else**
 - 35: Increment k by 1 and return to Step 3.
 - 36: **end if**
 - 37: **Output Results:**
 - 38: Display the optimal solution, which comprises the best positions (optimal DG locations and sizes), along with the corresponding fitness value indicating the minimum total active power loss.
-

The objective function of PSO technique is to minimize power losses.

$$\text{Minimize } P_L = \sum_{k=1}^n \text{Loss}_k. \quad (1)$$

Equations involved in PSO technique [14] are as follows:

$$v_i^{k+1} = cv_i^k + a_1b_1(pbest_i - s_i^k) + a_2b_2(gbest_i - s_i^k); \tag{2}$$

$$s_i^{k+1} = s_i^k + v_i^{k+1}, \tag{3}$$

where: a_1, a_2 are acceleration coefficients; b_1, b_2 are random numbers between 0 and 1; c is the weight assigned to each objective; n is the number of particles in a group; and v_i^k is the current velocity of particle 'i' at iteration 'k'.

2.5. Photovoltaics Integration in OpenDSS

The PV System model in OpenDSS combines solar PV array and inverter characteristics for distribution system studies is shown in Figure 3. It simplifies modeling by assuming effective maximum power point tracking within 1–5-h time steps. Functioning like a standard Power Conversion element, it seamlessly integrates with circuit models as a generator or load device, aiding efficient distribution system simulations. The active power (P) is determined by the irradiance, temperature (T), and rated power at the maximum power point (Pmpp, P*eff) under standard conditions (1.0 kW/m²). Inverter efficiency at the operating power and voltage is factored in. Reactive power is separately specified, either by fixed kVAR values or power factor. Arrays describe how Pmpp varies with temperature relative to the chosen rated Pmpp temperature. Additionally, an array represents the inverter efficiency curve, utilizing a single curve near the typical operating voltage of the array [14]. The PV system model in OpenDSS is used to simulate the performance of photovoltaic systems integrated into the distribution network. This model takes into account the measured solar irradiance data collected from Gudimangalam, Tamil Nadu, on 10 March 2018 as input. The variation in solar irradiance over the day is used to calculate the corresponding power output from the PV system at each time step using the PV system model equations.

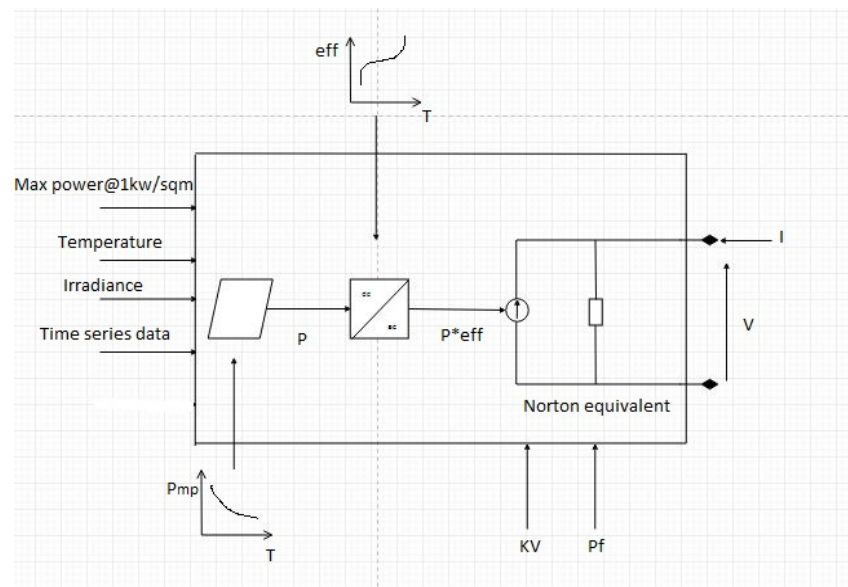


Figure 3. PV System model conceptual diagram.

On 10 March 2018, in Gudimangalam, Tamil Nadu, the maximum solar irradiance of 951.41 W/sq. m was recorded at 14:00 (2 pm) with a temperature of 31 °C. Minimum irradiance occurred at various intervals between 19:00 (7 pm) and 23:00 (11 pm), and between 01:00 (1 am) and 06:00 (6 am), with temperatures varying accordingly. Power output from the PV system was observed at different time periods throughout the day.

2.6. Wind Generator Integration in OpenDSS

The wind generator model in OpenDSS is utilized to simulate the behavior of wind power generators connected to the distribution network. The model takes into account the specifications and characteristics of the wind turbine. The power output calculations are based on the measured wind speed data collected from the study location, which captures the variability of wind resources throughout the day. The wind generator model in OpenDSS, depicted in Figure 4, steps up the output to network voltage and connects it at the optimal bus location determined by PSO. Time series data for wind speed on 28 March 2018 are collected for load flow analysis. The wind generator specifications are set according to the default generator model in OpenDSS [15]: Per unit stator resistance: 0.0053; Per unit stator leakage reactance: 0.106; Per unit rotor resistance: 0.007; Per unit rotor leakage reactance: 0.12.

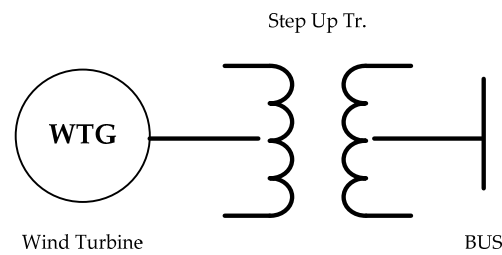


Figure 4. Wind system model.

Wind turbine specifications are taken from model V-90, with rated power output of 3 MW. To calculate wind power output. Equation (4) is used at a time step of 1 h for 24 h [16,17].

$$P_w = \frac{1}{2} * \rho * A * V^3 * C_p \tag{4}$$

Electrical Power output (P_w); Velocity of Wind speed (V); Swept Area (A) = 6362 m²; Power coefficient (C_p) = 0.59 (Maximum value); Air density (ρ) = 1.225 kg/m³.

2.7. Combined PV and Wind Integration

The OpenDSS model integrates a solar PV array model with inverter characteristics for distribution system impact assessments, accounting for wind energy and PV data in the computation of average power production, as depicted in Figure 5.

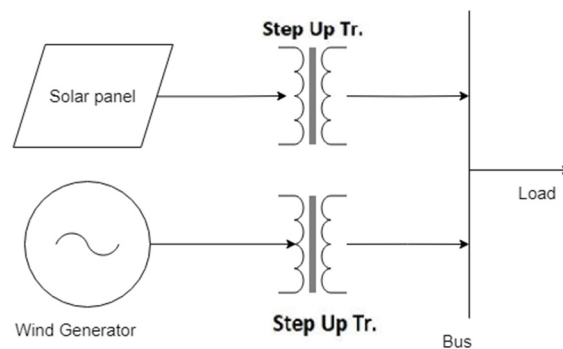


Figure 5. Circuit connection of both PV and wind.

3. Test System

This methodology is tested on a system containing 33 buses and 32 branches, as shown in Figure 6. It is a radial system with a total load of 3.72 MW and 2.3 MVAR.

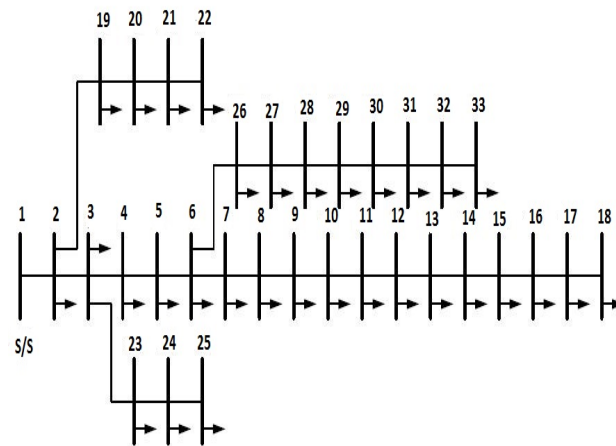


Figure 6. SLD of 33Bus distribution test system.

A MATLAB program is developed to determine the optimal size of distributed generation (DG) at different buses and estimate the total loss with DG at various locations to identify the best location using Particle Swarm Optimization (PSO). The program also analyzes the network voltage profile under different conditions, including PV, wind, and their integration.

4. Results and Discussion

4.1. Voltage Profile of 33 Bus System with and without DG Using Backward and Forward Sweep Algorithm

The voltage profile and power losses of the 33-bus radial distribution system were analyzed using the backward–forward sweep load flow algorithm. Figure 7 shows the voltage profile without any distributed generation (DG) connected to the network. It can be observed that several buses exhibit voltage magnitudes below the desired range of 0.95 to 1.05 per unit (p.u.), indicating potential issues with voltage regulation and power quality.

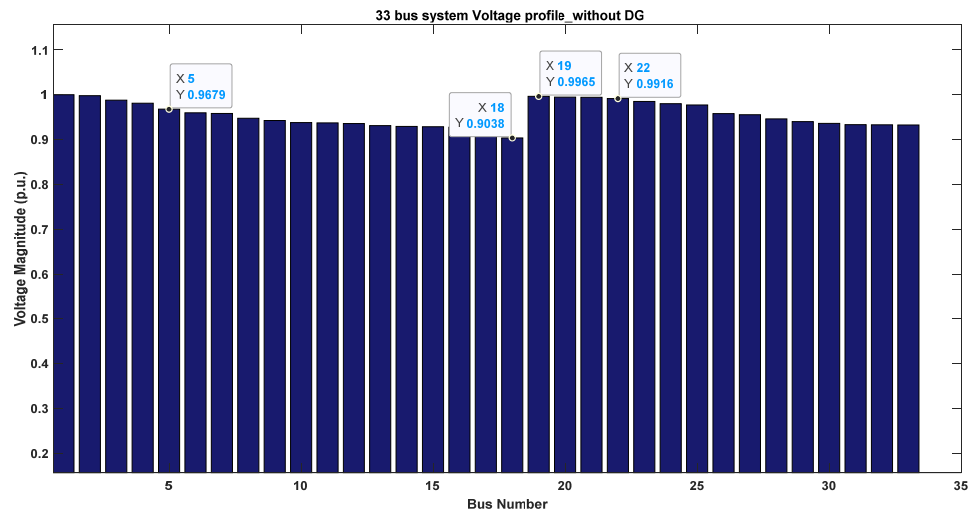


Figure 7. 33 BUS system Voltage profile without DG.

To address these concerns, the optimal location and size of DG were determined using Particle Swarm Optimization (PSO). The objective of the PSO algorithm was to minimize the total system power losses while ensuring that the bus voltages remain within the prescribed limits after DG integration. The optimal DG size was found to be 2910 kW, and the optimal location for DG placement was identified as Bus 7, presented in Table 1.

Table 1. Optimal location and size of DG.

Optimal DG Location	Bus 7
Optimal DG size	2910 kW

Figure 8 illustrates the voltage profile after connecting the optimal DG at Bus 7. A significant improvement in the voltage profile can be observed, with all bus voltages now maintained within the desired range of 0.95 to 1.05 p.u. This voltage regulation enhancement is crucial for ensuring power quality, reducing electrical losses, and maintaining the stable operation of the distribution network.

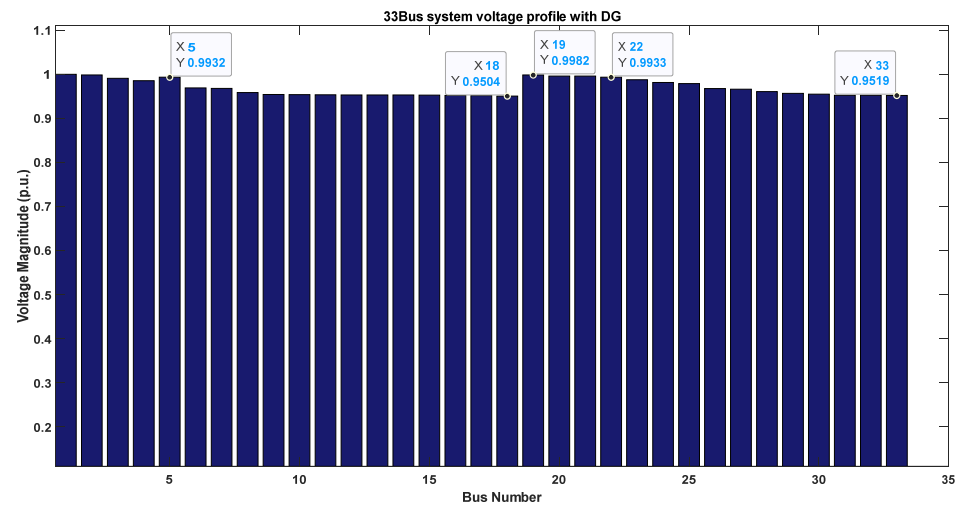


Figure 8. 33Bus system voltage profile with DG.

Table 2 quantifies the reduction in power losses achieved by integrating the optimal DG into the system. Without DG, the total real power loss was 210.987 kW, and the total reactive power loss was 143.1284 kVAR. After connecting the DG, these losses were reduced to 115.0820 kW and 91.2103 kVAR, respectively. This represents a substantial reduction of approximately 45.5% in real power losses and 36.3% in reactive power losses.

Table 2. Comparison of power loss with and without DG.

Connection	Total Real Power Loss (kW)	Total Reactive Power Loss (kVAR)
Without DG	210.987	143.1284
With DG	115.0820	91.2103

The reduction in power losses can be attributed to several factors, including the optimal sizing and placement of the DG, as well as the network configuration and loading conditions. By injecting active power at an optimal location, the DG effectively reduces the current flow through the distribution lines, thereby minimizing resistive losses. Additionally, the reactive power support provided by the DG helps to improve voltage regulation, further contributing to loss reduction.

4.2. Photovoltaics Integration

On 10 March 2018, the maximum irradiance of 951.41 W/sq. m was recorded at 13:00 h (1 pm), accompanied by a temperature of 31 °C. The corresponding PV output was 0.4348 MW. For the time intervals from 19:00 h to 23:00 h and from 01:00 h to 06:00 h, the PV power output was negligible, reaching 0 MW. This variation in PV power output is illustrated in Figure 9.

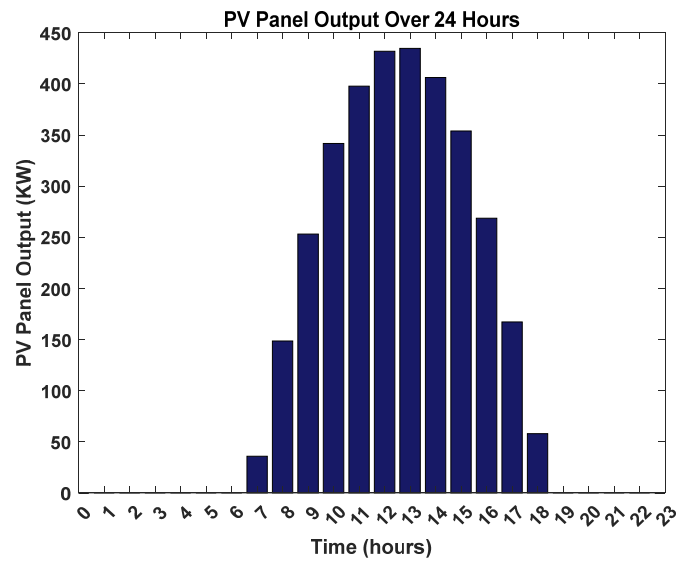


Figure 9. PV power output.

Figure 10 displays the system voltage profile plotted for the maximum PV output observed at 13:00 h (1 pm).

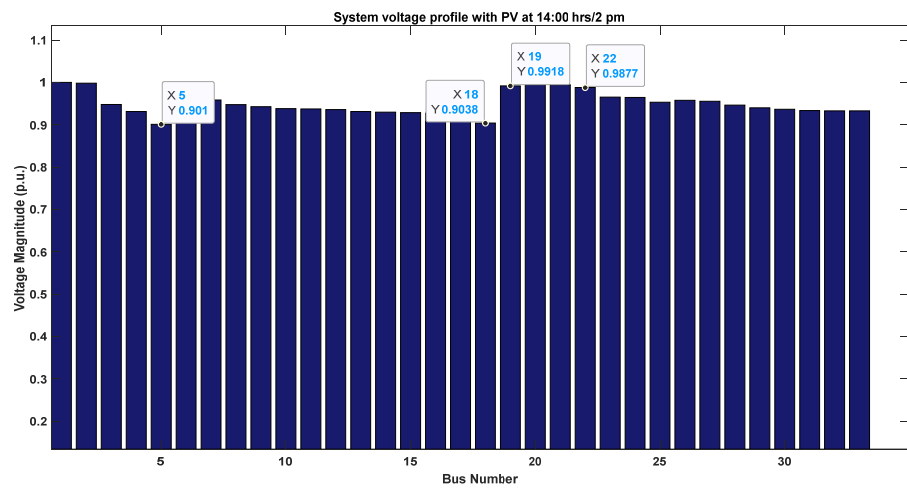


Figure 10. System voltage profile with PV.

The PV output is observed to be very low, resulting in minimal variation in the system voltage profile with and without PV.

4.3. Wind Generator Integration

Within a 24-h interval, the maximum wind speed was observed at 19:00 h (7 pm), reaching 10.81 m/s, with a corresponding wind power output of 2.904 MW. Conversely, the minimum wind speed was recorded at 01:00 h (1 am), with a velocity of 8.74 m/s and a corresponding wind power output of 1.53 MW. This variation is depicted in Figures 11, 12 and 13 respectively.

The system voltage profile at the maximum wind power output is depicted in Figure 14.

The maximum wind power output was recorded at 2.904 MW. Consequently, the system voltage profile with only wind generation exhibited a substantial improvement compared to the voltage profile with only solar output. However, despite this improvement, some system voltages still did not adhere to the prescribed limits.

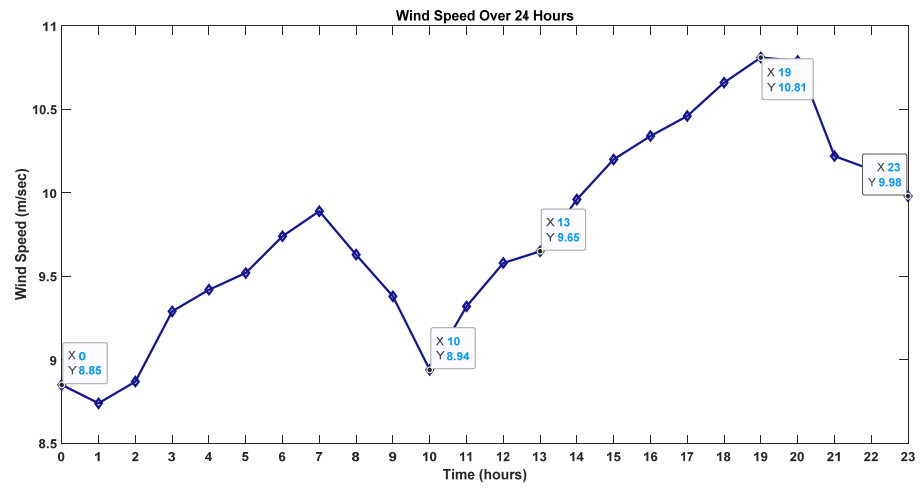


Figure 11. Wind speed vs. time.

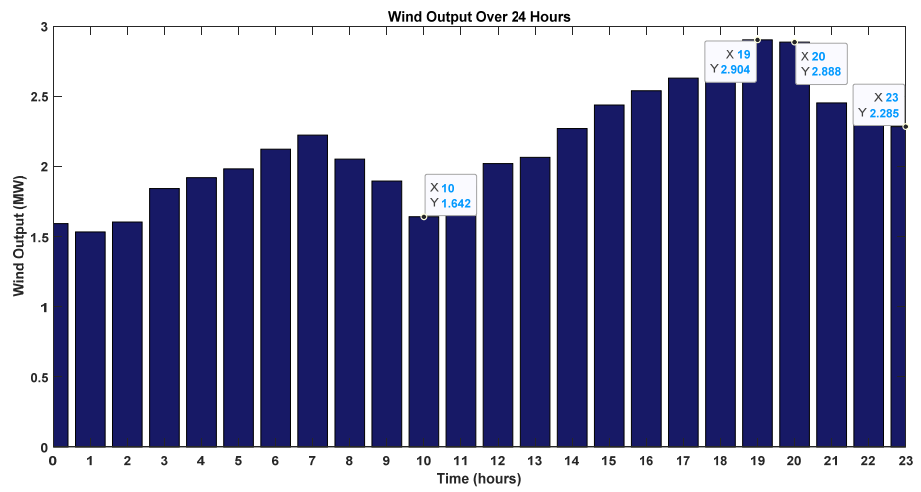


Figure 12. Wind power output.

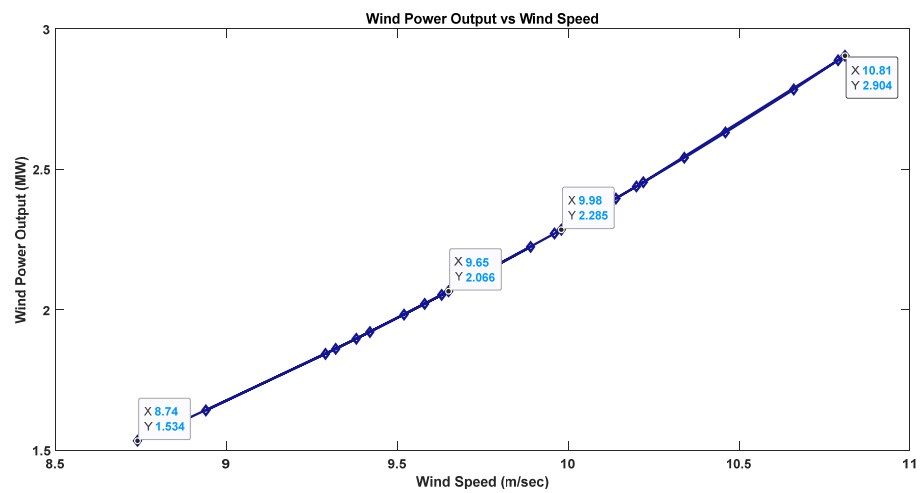


Figure 13. Wind power output vs. wind speed.

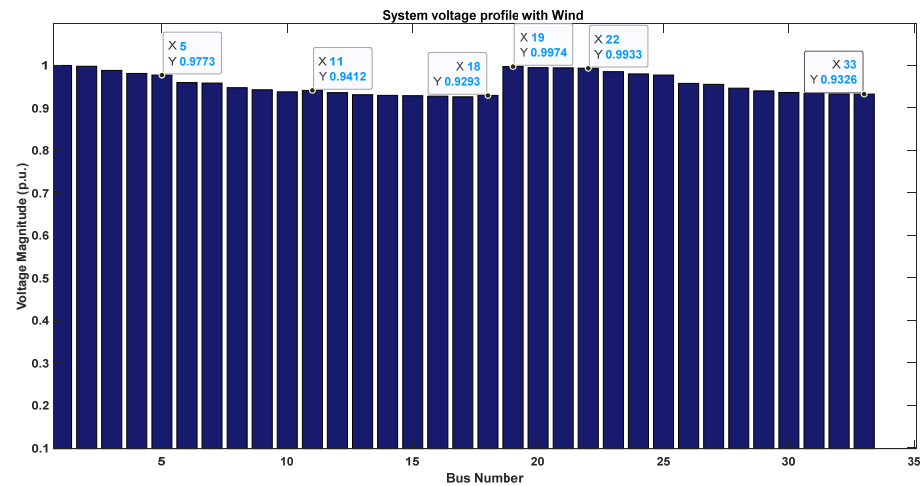


Figure 14. System voltage profile with wind power.

4.4. Combined PV and Wind Integration

On 16 April, the maximum solar irradiance was recorded at 14:00 h (2 pm), reaching 1120.56 W/sq. m. This coincided with a temperature of 35 °C. Conversely, the minimum PV power output was observed at various time intervals from 00:00 h to 05:00 h and from 20:00 h to 23:00 h, occurring at different temperatures as depicted in Figure 15.

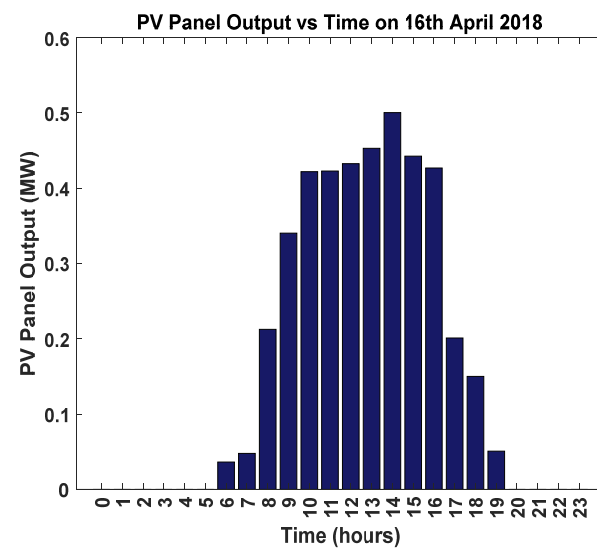


Figure 15. PV output power.

Wind speed data for 16 April 2018 have been recorded and will be combined with PV data. Figure 16 illustrates the variation in wind speed over time. The maximum wind speed occurred at 20:00 h (8 pm) with a velocity of 10.66 m/s, while the minimum wind speed was noted at 00:00 h (12 am) with a velocity of 8.10 m/s. This variation is depicted in Figure 16.

The wind power profile is depicted in Figure 17, where the maximum wind power output of 2.784 MW is recorded at 20:00 h (8 pm).

The minimum wind power output is determined to be 1.2218 MW, corresponding to the minimum wind speed observed at 00:00 h (12 am). Figure 18 illustrates the variation in wind power and wind speed over time. The total power output analysis with integration of PV and wind generation is shown in Table 3 as follows.

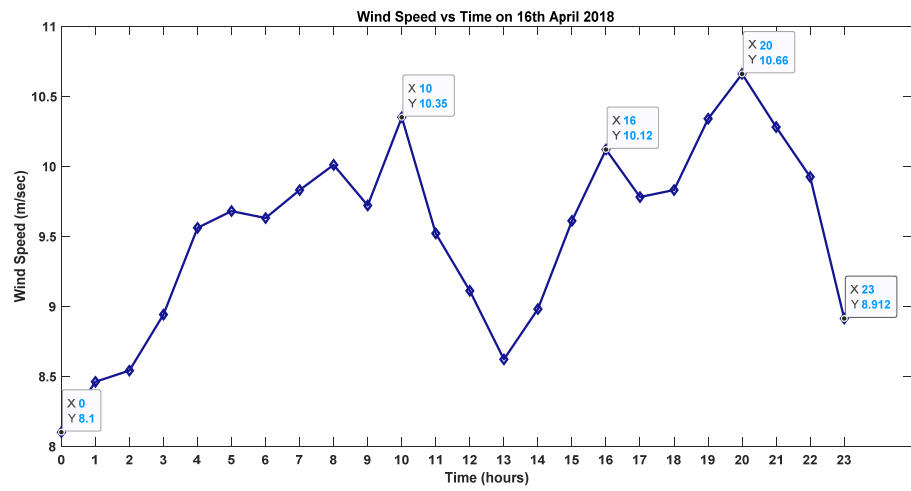


Figure 16. Wind speed vs. time.

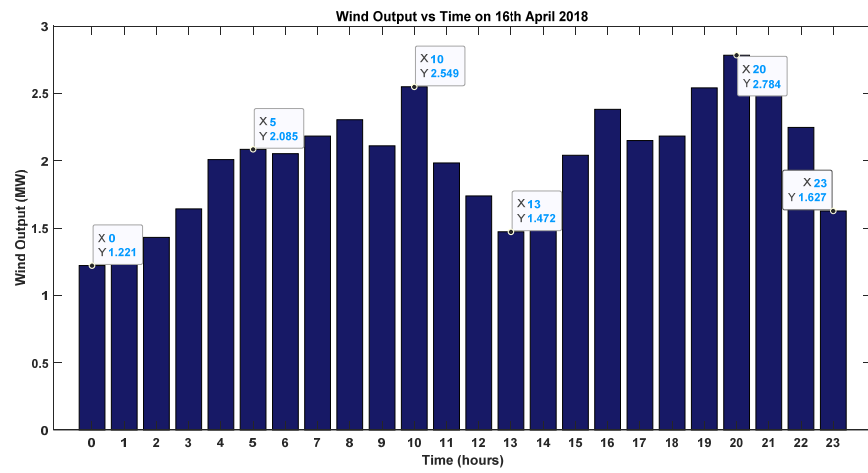


Figure 17. Wind power output.

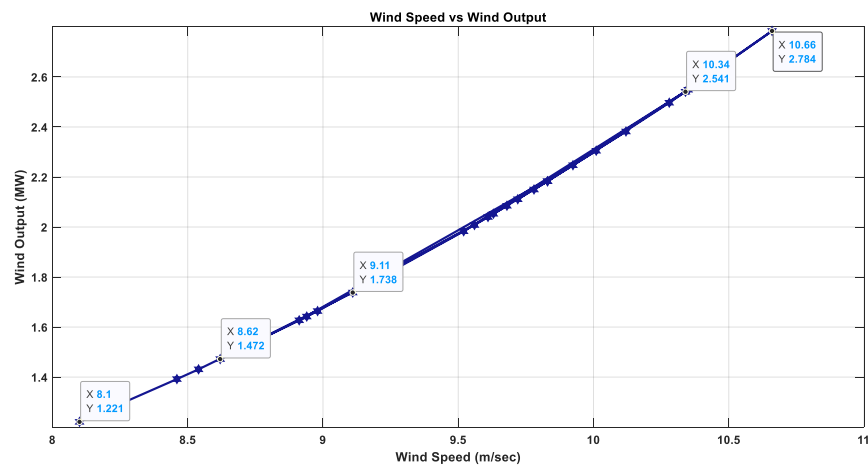


Figure 18. Wind power output vs. wind speed.

In combined PV and wind power generation, four distinct cases are considered.

Table 3. Total power output when combined PV and wind generation.

PV Panel O/p (MW)	Wind Output (MW)	Total Power (MW)
0	1.221	1.221
0	1.392	1.392
0	1.431	1.431
0	1.642	1.642
0	2.008	2.008
0	2.085	2.085
0.0364	2.053	2.089
0.0478	2.183	2.231
0.2126	2.305	2.518
0.3403	2.111	2.451
0.4218	2.549	2.970
0.4228	1.983	2.406
0.4326	1.7382	2.170
0.4529	1.472	1.925
0.5004	1.664	2.165
0.4425	2.040	2.482
0.4267	2.382	2.8087
0.201	2.150	2.351
0.15	2.183	2.333
0.0508	2.541	2.592
0	2.784	2.784
0	2.497	2.497
0	2.247	2.247
0	1.627	1.627

4.4.1. CASE 1: When Total Power Generated Is Minimum

On 16 April 2018, at 00:00 h (12 am), both solar irradiance and wind speed reached their minimum values, with solar irradiance being zero and wind speed at 8.1 m/s. Consequently, the power output from solar was 0 MW, while from wind it was 1.221 MW. Thus, the total power output amounted to 1.221 MW.

From Figure 19, it is evident that there is a need for additional power injection to sustain the system voltage profile within the prescribed limits.

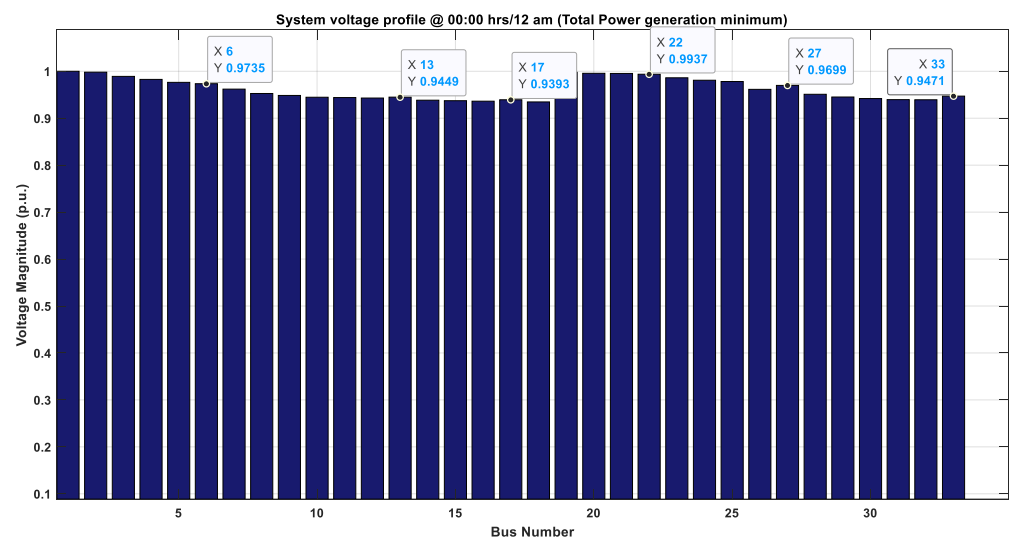


Figure 19. System voltage profile when total output power is minimum.

4.4.2. CASE 2: When Solar Power Generated Is Maximum

At 14:00 h (2 pm), solar irradiance reached its maximum value at 1120.56 W/sq. m, while the average wind speed was 8.98 m/s. The generated power from photovoltaic

(PV) and wind sources amounted to 0.5 MW and 1.6648 MW, respectively, resulting in a total distributed power generation of 2.1652 MW. Figure 20 displays the corresponding voltage profile.

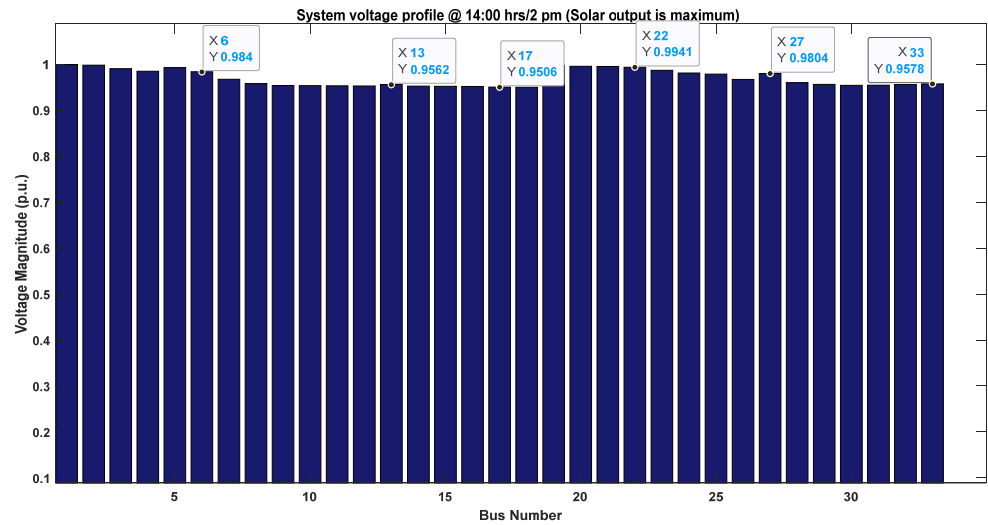


Figure 20. System voltage profile when solar output power is maximum.

In this scenario, there is a significant improvement in voltage compared to Case 1. This improvement can be attributed to the substantial wind generation observed at Gudimangalam at around 2 pm.

4.4.3. CASE 3: When Wind Power Generated Is Maximum

At 20:00 h (8 pm), the wind speed peaked at 10.66 m/s, while solar irradiance remained at zero. The output generated from wind was 2.784 MW, while solar output was negligible at 0 MW, resulting in a total power output of 2.784 MW. Figure 21 illustrates the voltage profile corresponding to the maximum wind output.

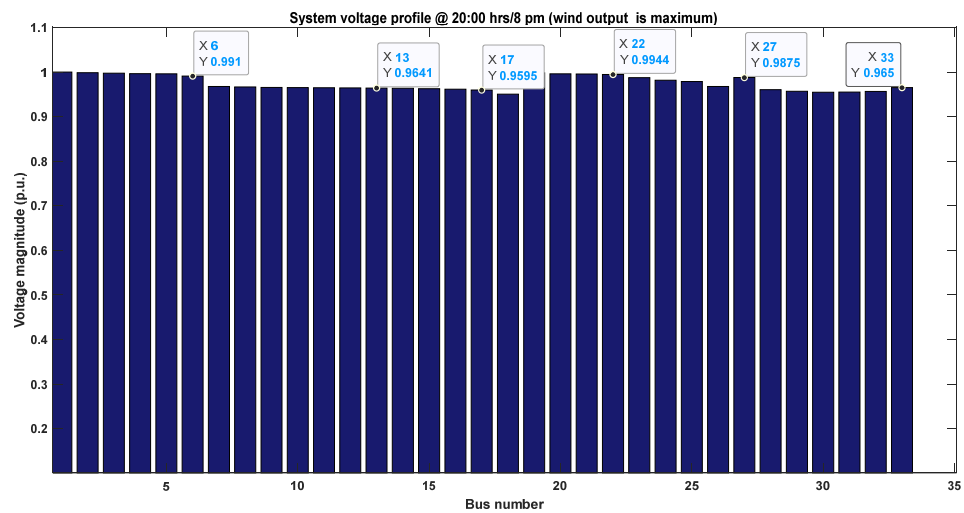


Figure 21. System voltage profile when wind output power is maximum.

At the time of wind power generation, it was observed that the generated power did not exceed the optimal value required. Consequently, some bus voltages were found to be outside the specified limits.

4.4.4. CASE 4: When Total Power Generated Is Maximum

At 10:00 h, the maximum total power generation at Gudimangalam, Tamil Nadu, was observed, coinciding with a solar irradiance of 896.45 W/sq. m and a wind speed of 10.19 m/s. The power generation from photovoltaic (PV) and wind sources amounted to 0.4218 MW and 2.4326 MW, respectively. Figure 22 illustrates the system voltage profile at this specific moment.

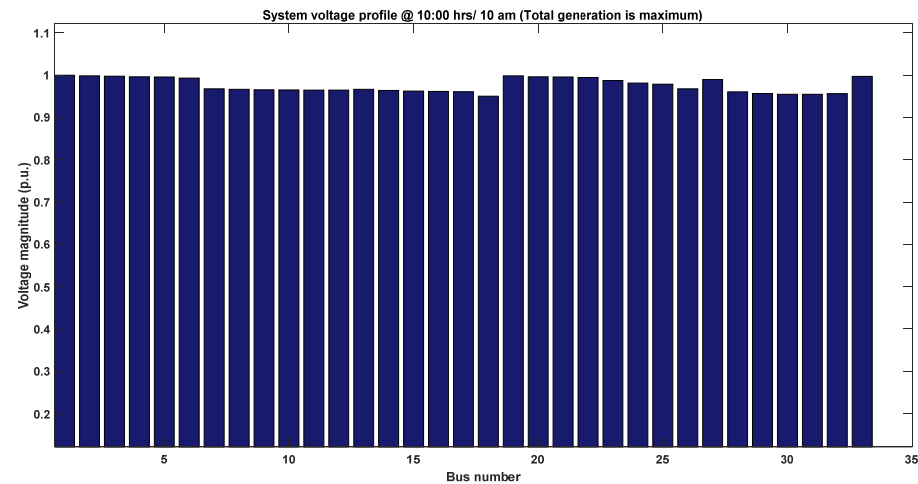


Figure 22. System voltage profile when total output power is maximum.

By 10 am, the total power generation exceeds the optimal size of distributed generation. Nevertheless, all bus voltages are successfully maintained within their prescribed limits.

5. Conclusions

This study presents a robust methodology for accurately estimating the actual power output from renewable energy sources, specifically focusing on solar and wind energy, using time series data collected from Gudi-Mangalam, Tamil Nadu. By integrating this data into the IEEE 33-Bus radial distribution network in various scenarios, including solar-only, wind-only, and combined solar–wind configurations, the study offers insights into the potential impact of renewable energy integration on distribution system operations. Through time series simulations conducted using the OpenDSS software interfaced with MATLAB, the study evaluates the performance of the distribution network with renewable energy integration. The primary objective is to maximize the total real power loss reduction within the distribution system while ensuring voltage limits are maintained post-connection of distributed generation (DG). Utilizing the Particle Swarm Optimization (PSO) algorithm, the study identifies renewable energy sources' optimal location and size to achieve the desired objectives. By optimizing the placement and capacity of solar and wind sources, the study demonstrates the potential for significant improvements in distribution system efficiency and reliability. The findings highlight the importance of proper planning and optimization in integrating renewable energy sources into distribution networks. Utilities can enhance system performance, reduce losses, and contribute to the transition towards a more sustainable energy future by accurately estimating power output and strategically placing renewable generation.

Author Contributions: Conceptualization, S.T. and D.N.G.; methodology, S.T. and R.S.; software, A.S.V. and S.T.; validation, A.S.V., D.N.G. and R.S.; formal analysis, S.T.; investigation, A.S.V. and S.T.; resources, S.T.; data curation, A.S.V. and S.T.; writing—original draft preparation, S.T.; writing—review and editing, R.S., D.N.G. and A.S.V.; visualization, A.S.V. and S.T.; supervision, D.N.G. All authors have read and agreed to the published version of the manuscript.

Funding: This research received no external funding.

Institutional Review Board Statement: Not applicable.

Informed Consent Statement: Not applicable.

Data Availability Statement: The data that support the findings of this study are available from the corresponding author upon reasonable request.

Conflicts of Interest: The authors declare no conflicts of interest.

References

1. Prema, V.; Rao, K.U. Development of statistical time series models for solar power prediction. *Renew. Energy* **2015**, *83*, 100–109. [[CrossRef](#)]
2. Prema, V.; Rao, K.U. Time series decomposition model for accurate wind speed forecast. *Renew. Wind Water Solar* **2015**, *2*, 18. [[CrossRef](#)]
3. Rupa, J.M.; Ganesh, S. Power flow analysis for radial distribution system using backward/forward sweep method. *Int. J. Electr. Comput. Electron. Commun. Eng.* **2014**, *8*, 1540–1544.
4. Noureddine, T.; Djamel, L. Load flow analysis using Newton-Raphson method in presence of distributed generation. *Int. J. Power Electron. Drive Syst.* **2021**, *12*, 489. [[CrossRef](#)]
5. Hossain, F.A.; Rokouzzaman, M.; Amin, N.; Zhang, J.; Mishu, M.K.; Tan, W.-S.; Islam, M.R.; Roy, R.B. Probabilistic Load Flow-Based Optimal Placement and Sizing of Distributed Generators. *Energies* **2021**, *14*, 7857. [[CrossRef](#)]
6. Meskin, M.; Domijan, A.; Grinberg, I. Impact of distributed generation on the protection systems of distribution networks: Analysis and remedies—review paper. *IET Gener. Transm. Distrib.* **2020**, *14*, 5944–5960. [[CrossRef](#)]
7. Venkatesan, Y.; Pandian, A.N.; Palanivelu, A. A simple and efficient power flow for distribution networks. *Technol. Econ. Smart Grids Sustain. Energy* **2022**, *7*, 10. [[CrossRef](#)]
8. Tyagi, A.; Kumar, K.; Ansari, M.A.; Kumar, B. An efficient load flow solution for distribution system with addition of distributed generation using improved harmony search algorithms. *J. Electr. Syst. Inf. Technol.* **2020**, *7*, 7. [[CrossRef](#)]
9. Uruel-Sanz, J.; Perpiñán-Lamigueiro, O. Power Flow Analysis in Urban Distribution Networks with Implementation of Grid-Connected Photovoltaic Systems. *Solar* **2022**, *2*, 32–51. [[CrossRef](#)]
10. Bompard, E.; Carpaneto, E.; Chicco, G.; Napoli, R. Convergence of the backward/forward sweep method for the load-flow analysis of radial distribution systems. *Int. J. Electr. Power Energy Syst.* **2000**, *22*, 521–530. [[CrossRef](#)]
11. Rana, A.D.; Darji, J.B.; Pandya, M. Backward/forward sweep load flow algorithm for radial distribution system. *Int. J. Sci. Res. Dev.* **2014**, *2*, 398–400.
12. Bhumkittipich, K.; Phuangsornpitak, W. Optimal placement and sizing of distributed generation for power loss reduction using particle swarm optimization. *Energy Procedia* **2013**, *34*, 307–317. [[CrossRef](#)]
13. Sharma, P.; Tandon, A. Techniques for optimal placement of DG in radial distribution system: A review. In Proceedings of the 2015 Communication, Control and Intelligent Systems (CCIS), Mathura, India, 7–8 November 2015; pp. 453–458. [[CrossRef](#)]
14. Smith, J.W.; Dugan, R.; Sunderman, W. Distribution modeling and analysis of high penetration PV. In Proceedings of the 2011 IEEE Power and Energy Society General Meeting, Detroit, MI, USA, 24–29 July 2011; pp. 1–7. [[CrossRef](#)]
15. Dugan, R.C.; Montenegro, D. *The Open Distribution System Simulator (OpenDSS): Reference Guide*; Electric Power Research Institute (EPRI): Washington, DC, USA, 2018.
16. Manyonge, A.W.; Ochieng, R.M.; Onyango, F.N.; Shichikha, J.M. Mathematical modelling of wind turbine in a wind energy conversion system: Power coefficient analysis. *Appl. Math. Sci.* **2012**, *6*, 4527–4536.
17. Adepoju, G.A.; Aderemi, B.A.; Salimon, S.A.; Alabi, O.J. Optimal placement and sizing of distributed generation for power loss minimization in distribution network using particle swarm optimization technique. *Eur. J. Eng. Technol. Res.* **2023**, *8*, 19–25. [[CrossRef](#)]

Disclaimer/Publisher’s Note: The statements, opinions and data contained in all publications are solely those of the individual author(s) and contributor(s) and not of MDPI and/or the editor(s). MDPI and/or the editor(s) disclaim responsibility for any injury to people or property resulting from any ideas, methods, instructions or products referred to in the content.